Nuclear Instruments and Methods in Physics Research B 361 (2015) 659–664

Contents lists available at ScienceDirect

Nuclear Instruments and Methods in Physics Research B

journal homepage: www.elsevier.com/locate/nimb

# A high resolution method for $^{14}C$ analysis of a coral from South China Sea: Implication for "AD 775" $^{14}C$ event

Ping Ding [a], Chengde Shen [a,b,*], Weixi Yi [a], Ning Wang [a], Xingfang Ding [b], Kexin Liu [b], Dongpo Fu [b], Weiguo Liu [c], Yi Liu [d]

[a] State Key Laboratory of Isotope Geochemistry, Guangzhou Institute of Geochemistry, Chinese Academy of Sciences, 510640 Guangzhou, China
[b] State Key Laboratory of Nuclear Physics and Technology, Peking University, 100871 Beijing, China
[c] State Key Laboratory of Loess and Quaternary Geology, Institute of Earth Environment, The Chinese Academy of Sciences, 710075 Xi'an, China
[d] CAS Key Laboratory of Crust-Mantle Materials and Environments, School of Earth and Space Sciences, University of Science and Technology of China, 230026 Hefei, China

ARTICLE INFO

*Article history:*
Received 15 December 2014
Received in revised form 25 June 2015
Accepted 25 June 2015
Available online 9 July 2015

*Keywords:*
Pre-heating
Coral
Bi-weekly resolution
AD 776
$^{14}C$ spike

ABSTRACT

A pre-heating method that improves the background and precision of $^{14}C$ dating significantly was applied for fossil coral dating with high resolution in our lab in Guangzhou Institute of Geochemistry, Chinese Academy of Sciences (GIGCAS). The reaction tube is heated under 300 °C in a vacuum line before it is used for graphitization. The method can reduce the contamination absorbed in $TiH_2$, Zn and Fe power placed in the graphitization tube. With the pre-heating and average drilling method, bi-weekly resolution $^{14}C$ dating in a fossil coral is carried out to investigate the "AD 775 $^{14}C$ spike event". Different from the tree ring $^{14}C$ archives with the $^{14}C$ spike of ~15‰ ($\Delta^{14}C$), the $^{14}C$ spike in the coral shows an abrupt peak of 45‰ and two smaller spikes of $\Delta^{14}C > 20$‰ in half a year in AD 776. And then, the $^{14}C$ content in coral decreases gradually in AD 777. The peak time of the $^{14}C$ spike event likely occurs in the summer of AD 776 according to the $\delta^{18}O$ variation in coral. High-resolution dating of $^{14}C$ in coral provides not only a more detail process of the event than that from tree rings, but also the first report of the event from sea ecosystem. Both of them suggest an extraterrestrial origin of the event cause.



## 1. Introduction

Radiocarbon ($^{14}C$) is primarily formed through the reaction of cosmic rays and atmospheric nitrogen. The pulse of the atmospheric $^{14}C$ content could be documented in coral through air–sea $CO_2$ gas exchange and biogeochemical cycle in the sea [1]. Different from annual resolution record in the tree ring, coral provides seasonal, monthly or even weekly resolution [2]. Sometimes, annual resolution is not high enough to show the course of an abrupt event clearly, such as "AD 775" cosmogenic ray enrichment event [3,4]. To find out the true cause, *e.g.*, contribution by a long-period comets collision [4–6], a galactic short gamma-ray burst [7], or a proton storm from giant solar flares [8–10], for an unexpectable burst of atmospheric $^{14}C$, higher resolution than annual dating of $^{14}C$ in coral would be helpful. At present, monthly resolution of $^{14}C$ in coral is the highest among which has been reported [11]. For a higher resolution dating of $^{14}C$ in coral, such as biweekly resolution, precision of $^{14}C$ dating is important to note because the amount of available sample is usually limited and the amplitude of fluctuation is usually low.

In this paper we introduce a pre-heating method that used in the preparation of $^{14}C$ dating with AMS in AMS-$^{14}C$ lab in Guangzhou Institute of Geochemistry, Chinese Academy of Sciences (GIGCAS). Using this method, a fossil *Porites* coral that covering the "AD 775" event is subsampled by average drilling and dated by $^{14}C$ in biweekly resolution. The core of fossil *Porites* coral is drilled from Xiaodonghai (XDH) Reef in the northern South China Sea in 1997. It is cut into slabs of 7 mm in thickness with 1.2 m long. X-ray diffraction analysis shows the coral is 100% aragonite and scanning electron microscopy image indicates the absence of secondary aragonite along the slab. The coral was dated by $^{230}Th$ techniques at the High-Precision Mass Spectrometry and Environment Change Laboratory (HISPEC), National Taiwan University, on a multi-collector inductively coupled plasma mass spectrometer (MC-ICP-MS), giving an age of AD 776 ± 14 at the depth of 11.6 cm [4].

* Corresponding author at: State Key Laboratory of Isotope Geochemistry, Guangzhou Institute of Geochemistry, Chinese Academy of Sciences, 510640 Guangzhou, China.
*E-mail address:* cdshen@gig.ac.cn (C. Shen).

http://dx.doi.org/10.1016/j.nimb.2015.06.032
0168-583X/

## 2. Materials and methods

### 2.1. Materials

The coral was separated into biweekly-resolution subsamples by average drilling vertically at depths of 12.25–17.19 cm (Table 1). The surface of coral was polished firstly, and then drilled along the growth axis in a same interval of 0.1 cm. Table 1 shows the detail separating depth. It covered 2 years when the $^{14}C$ content in coral increased abnormally [4]. The coral is dated by $^{230}Th$ at a depth of 2.15 cm, giving an age of AD 783 ± 14, which is 7 annual growth bands above the layer containing the onset of $^{14}C$ anomalies at a depth of 16.11 cm and corresponding to an age of AD 776 ± 14 [4]. About 6–8 mg coral power was obtained for each subsample. At the depth 12.70 cm, 13.78 cm, 15.03 cm, 15.93 cm of the coral, we separated the subsample with the amount of about 3 mg for the duplication measurement (Table 1).

**Table 1**
Details of the biweekly interval data.

| Sample No. | Depth (cm) | Year[a] (AD) | $\Delta^{14}C$ (‰) | Uncertainty (±) | $\delta^{18}O$ (‰) | $\delta^{13}C$ (‰) |
|---|---|---|---|---|---|---|
| XDH-m-1 | 12.25 | 777 | −182.0 | 2.5 | −4.60 | −1.98 |
| XDH-m-2 | 12.34 | 777 | −180.8 | 2.5 | −4.76 | −1.78 |
| XDH-m-3 | 12.43 | 777 | −180.0 | 2.4 | −5.52 | −1.88 |
| XDH-m-4 | 12.52 | 777 | −180.2 | 3.2 | −5.35 | −2.38 |
| XDH-m-5 | 12.61 | 777 | −182.1 | 2.8 | −5.16 | −2.51 |
| XDH-m-6 | 12.70 | 777 | −179.2 | 3.0 | −5.22 | −2.41 |
| XDH-m-6′ | 12.70 | 777 | −181.4 | 2.8 | | |
| XDH-m-7 | 12.79 | 777 | −183.3 | 2.5 | −5.03 | −1.99 |
| XDH-m-8 | 12.88 | 777 | −171.9 | 2.5 | −4.8 | −1.88 |
| XDH-m-9 | 12.97 | 777 | −181.3 | 3.1 | −4.98 | −2.18 |
| XDH-m-10 | 13.06 | 777 | −179.1 | 2.6 | −4.81 | −2.04 |
| XDH-m-11 | 13.15 | 777 | −173.5 | 2.6 | −4.84 | −1.72 |
| XDH-m-12 | 13.24 | 777 | −177.3 | 3.0 | −4.87 | −1.74 |
| XDH-m-13 | 13.33 | 777 | −175.0 | 2.6 | −4.92 | −1.71 |
| XDH-m-14 | 13.42 | 777 | −170.6 | 2.7 | −5.12 | −1.57 |
| XDH-m-15 | 13.51 | 777 | −168.5 | 2.8 | −5.23 | −1.57 |
| XDH-m-16 | 13.60 | 777 | −175.6 | 2.4 | −5.37 | −1.36 |
| XDH-m-17 | 13.69 | 777 | −179.3 | 2.6 | −5.35 | −1.30 |
| XDH-m-18 | 13.78 | 777 | −173.7 | 2.6 | −5.53 | −1.35 |
| XDH-m-18′ | 13.78 | 777 | −175.9 | 2.8 | | |
| XDH-m-19 | 13.87 | 777 | −173.9 | 2.4 | −5.27 | −1.52 |
| XDH-m-20 | 13.96 | 777 | −179.8 | 3.0 | −5.38 | −1.77 |
| XDH-m-21 | 14.05 | 777 | −181.2 | 2.6 | −4.67 | −1.51 |
| XDH-m-22 | 14.14 | 777 | −177.0 | 2.7 | −4.51 | −1.48 |
| XDH-m-23 | 14.23 | 777 | −172.1 | 2.6 | −4.35 | −1.65 |
| XDH-m-24 | 14.32 | 777 | −174.4 | 2.4 | −4.31 | −1.08 |
| XDH-m-25 | 14.41 | 777 | −182.0 | 2.5 | −4.48 | −1.64 |
| XDH-m-26 | 14.50 | 776 | −178.2 | 2.4 | −4.59 | −1.47 |
| XDH-m-27 | 14.59 | 776 | −176.5 | 3.0 | −4.87 | −1.43 |
| XDH-m-28 | 14.67 | 776 | −175.4 | 2.8 | −4.55 | −1.36 |
| XDH-m-29 | 14.76 | 776 | −176.5 | 2.7 | −5.13 | −1.13 |
| XDH-m-30 | 14.85 | 776 | −175.6 | 2.5 | −5.21 | −1.22 |
| XDH-m-31 | 14.94 | 776 | −182.0 | 2.8 | −5.32 | −1.24 |
| XDH-m-32 | 15.03 | 776 | −145.6 | 2.4 | −5.13 | −1.11 |
| XDH-m-32′ | 15.03 | 776 | −148.8 | 2.6 | | |
| XDH-m-33 | 15.12 | 776 | −156.7 | 2.4 | −5.44 | −1.32 |
| XDH-m-34 | 15.21 | 776 | −168.8 | 2.4 | −5.01 | −1.63 |
| XDH-m-35 | 15.30 | 776 | −170.3 | 2.6 | −5.33 | −1.73 |
| XDH-m-36 | 15.39 | 776 | −175.5 | 3.0 | −5.23 | −1.56 |
| XDH-m-37 | 15.48 | 776 | −169.8 | 2.5 | −5.42 | −1.49 |
| XDH-m-38 | 15.57 | 776 | −179.1 | 2.5 | −5.43 | −1.10 |
| XDH-m-39 | 15.66 | 776 | −173.8 | 2.6 | −5.73 | −0.51 |
| XDH-m-40 | 15.75 | 776 | −142.9 | 2.4 | −5.51 | −1.19 |
| XDH-m-41 | 15.84 | 776 | −169.3 | 2.5 | −5.45 | −2.09 |
| XDH-m-42 | 15.93 | 776 | −148.7 | 2.4 | −5.12 | −1.38 |
| XDH-m-42′ | 15.93 | 776 | −146.4 | 2.5 | | |
| XDH-m-43 | 16.02 | 776 | −123.3 | 3.0 | −5.01 | −1.53 |
| XDH-m-44 | 16.11 | 776 | −164.0 | 2.5 | −5.23 | −1.30 |
| XDH-m-45 | 16.20 | 776 | −172.7 | 2.4 | −5.13 | −1.24 |
| XDH-m-46 | 16.29 | 776 | −173.5 | 2.4 | −4.85 | −1.35 |
| XDH-m-47 | 16.38 | 776 | −176.1 | 3.1 | −4.91 | −1.45 |
| XDH-m-48 | 16.47 | 776 | −177.0 | 2.8 | −4.60 | −1.37 |
| XDH-m-49 | 16.56 | 776 | −174.9 | 2.6 | −4.55 | −1.30 |
| XDH-m-50 | 16.65 | 776 | −173.3 | 2.6 | −4.35 | −1.35 |
| XDH-m-51 | 16.74 | 776 | −181.5 | 3.2 | −4.27 | −1.43 |
| XDH-m-52 | 16.83 | 776 | −178.0 | 2.6 | −4.44 | −1.42 |
| XDH-m-53 | 16.92 | 776 | −175.4 | 2.5 | −4.55 | −1.33 |
| XDH-m-54 | 17.01 | 775 | −189.8 | 2.5 | −4.82 | −1.18 |
| XDH-m-55 | 17.10 | 775 | −190.3 | 3.0 | −5.21 | −1.19 |
| XDH-m-56 | 17.19 | 775 | −190.7 | 2.4 | −5.57 | −1.02 |

[a] The chronology is based on $^{230}Th$ age of XDH-2 at the depth 2.15 cm and annual density bands of coral.

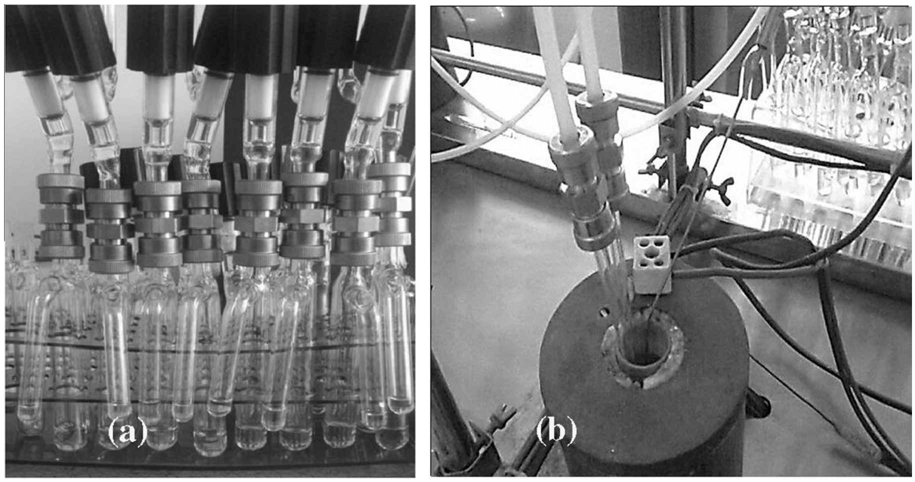


**Fig. 1.** Reaction tubes (a) and pre-heating oven (b).

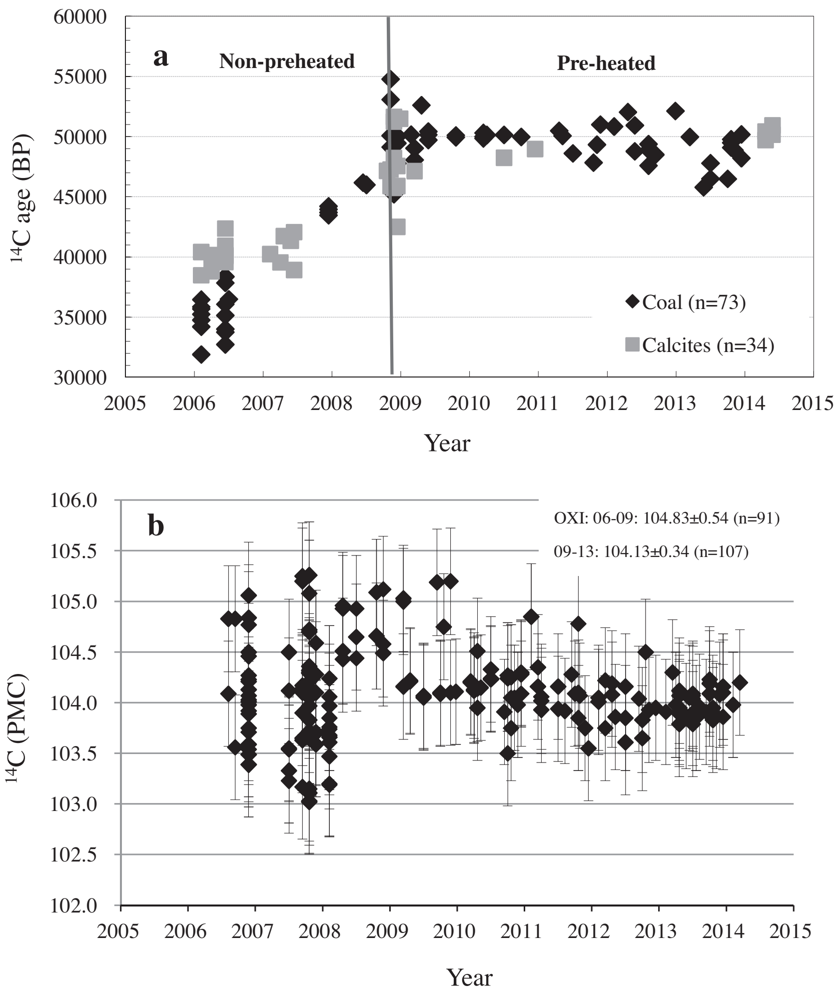


**Fig. 2.** Comparison of the $^{14}C$ data between the pre-heated and none pre-heated background (a, coal and calcites) and modern carbon standard OXI (b). The coal was pre-heated under 300 °C in the vacuum line for 6 h before it was changed into $CO_2$.

## *2.2. Method*

The detail chemical procedure is descripted as follow. Guaranteed reagent Phosphoric acid ($H_3PO_4$, >85%) was further purified under 60 °C in a vacuum drying oven for 72 h in order to make sure the purity of $H_3PO_4$ close to 100%. Reaction tube which has a branch was firstly sink with 0.5 mol/L HCl for 12 h and then rinsed with distilled water and dried in the vacuum drying oven. About 5 mg coral powder was weighted and placed into the reaction tube with purified $H_3PO_4$ in the branch. Tube was pumped in a vacuum system under $1.0 \times 10^{-3}$ Torr for at least 2 h before the sample was mixed with $H_3PO_4$. Graphitization tubes were cleaned in an ultrasound cleaner with distilled water, and then were dried in the vacuum drying oven. Finally, tubes were baked in an oven under 600 °C for 4 h. About 31.0 ± 0.5 mg Zn powder, 15.0 ± 0.5 mg $TiH_2$ powder, and 4.0 ± 0.2 mg Fe powder was placed into the graphitization tube. The graphitization tube is a 9 mm O.D. Pyrex reactor tube with reductants zinc and titanium hydride in bottom and catalyst iron in a 6 mm O.D. Pyrex culture tube sitting on a dimple 2 cm from the base of the outside tube.

Released $CO_2$ was extracted in a vacuum system and frozen to the graphitization tube. And then the graphitization tube was sealed by a torch. The total length of the sealed tube was 90 mm long. A shorter tube may be helpful for graphitization of smaller samples [12]. The $CO_2$ gas finally reduced to graphite using the method proposed by Xu et al. [13]. In order to reduce the contaminant involved in the $TiH_2$, Zn or Fe powder in the graphitization tube, pre-heating method was adopted. The graphitization tube was vacuumed first and then heated in the vacuum line under 300 °C in a smart oven fixed in the vacuum system for 15 min before the purified $CO_2$ was frozen inside (Fig. 1).

Graphite samples were analyzed in the AMS laboratory at Peking University. The standard used during the analysis was NIST-OXI, and the secondary modern carbon standard NIST-OXII was adopted. Two calcite samples pretreated as coral were used as background. The precision for $^{14}C$ analysis is about 3‰. It is important to mention that some of background and OXI data discussed in the pre-heating method section were analyzed in UC, Irvine, USA. Coral $\delta^{18}O$ measurements from the same biweekly subsamples were carried out with MAT-252 mass spectrometry equipped with Kiel II micro carbonate automatic sample input device at the Institute of Earth Environment, CAS. Results are reported as $\delta^{18}O$ and $\delta^{13}C$ with the international Vienna Pee Dee belemnite (PDB) standard. The analytical error of the laboratory standard is approximately ±0.2‰. $\delta^{18}O$ and $\delta^{13}C$ were not analyzed for the duplicated samples.

## 3. Results and discussion

### 3.1. Pre-heating method

We started the pre-heating method at the end of 2008. It was inspired by the two-step heating for organic carbon (OC) and element (EC), in which the volatile organic compounds could be removed [14]. It was helpful to improve the background and precision of $^{14}C$ dating in the AMS-$^{14}C$ lab in GIG-CAS. Fig. 2 shows the differences in background and modern carbon standard (OXI) between pre-heated graphitization tubes and none pre-heated tubes. The background improved gradually from 32 ka BP to 45 ka BP from 2006 to 2009 when graphitization tubes were not pre-heated. From 2009 to 2014, when the graphitization tube was pre-heated, the background climbed to older than 46 ka BP (Fig. 2). Besides pre-heating of graphitization tube, the coal was also pre-heated under 300 °C for 6 h in a vacuum line before it was oxidized into $CO_2$ gas. The mean value of PMC of OXI was 104.83 ± 0.54 ($n$ = 91) during 2006–2009, while it was improved to 104.13 ± 0.34 ($n$ = 107) during 2009–2014 when the pre-heating method was adopted. The international consensus value of PMC of OXI is about 104.00 in 2013, and the contemporaneous value in our lab is 104.00 ± 0.14 ($n$ = 32).

The effect of pre-heating method was not so significant in clean $^{14}C$ labs. Xu et al. [15] has compared the pre-heated and none pre-heated graphitization tubes in UCI, America. She found that there was no significant difference in results, but this method was useful for improving inhomogenous radiocarbon standards, such as Chinese sugar carbon [15]. The method can reduce the amount of volatile organic compounds absorbed in Fe, $TiH_2$, Zn powder and sample itself especially in the lab in heave air pollution areas.

Using the preheating method, the four duplications give very close $\Delta^{14}C$ values with the corresponding ones (Table 1). Standard deviations of the four duplicated samples at the depth 12.70 cm, 13.78 cm, 15.03 cm, 15.93 cm are 0.57‰, 1.56‰, 2.26‰ and 1.63‰, respectively, which are within the range of $^{14}C$ dating error 2.40–3.00‰.

### 3.2. Bi-weekly resolution of coral $\Delta^{14}C$

In order to find out the $^{14}C$ spike event recorded by the coral, the coral was first examined in half-annual resolution (Table 2). Results showed that the $^{14}C$ content increased from −188‰ to −177‰ when the event onset (Fig. 3a). The bi-weekly resolution of $\Delta^{14}C$ results shows that the $^{14}C$ content increases by ~15‰ during the winter to the early spring in AD 776, and remains elevated for more than 4 months (Fig. 3b). Then, it drops down in the following 1 month, forming a spike of 45‰ (S1) in late spring of AD 776. Another two smaller $^{14}C$ spikes ($\Delta^{14}C$ > 20‰, S2 and S3) occurs in the fo1lowing 5 months. Finally, the $^{14}C$ content in coral

**Table 2**
Details of the half-annual interval data.

| Sample No. | Depth (cm) | Year[a] (AD) | $\Delta^{14}C$ (‰) | Uncertainty (±) |
|---|---|---|---|---|
| XDH-1 | 1.04 | 783.5 | −184.1 | 2.4 |
| XDH-2 | 2.15 | 783.0 | −165.9 | 2.6 |
| XDH-3 | 2.99 | 782.5 | −176.8 | 2.4 |
| XDH-4 | 4.20 | 782.0 | −182.6 | 2.5 |
| XDH-5 | 5.22 | 781.5 | −175.1 | 3.0 |
| XDH-6 | 6.53 | 781.0 | −180.2 | 2.5 |
| XDH-7 | 7.53 | 780.5 | −172.1 | 3.0 |
| XDH-8 | 8.72 | 780.0 | −177.6 | 2.5 |
| XDH-9 | 9.59 | 779.5 | −179.8 | 2.4 |
| XDH-10 | 11.10 | 779.0 | −179.9 | 2.8 |
| XDH-11 | 12.31 | 778.5 | −175.0 | 3.1 |
| XDH-12 | 13.27 | 778.0 | −175.5 | 2.8 |
| XDH-13 | 14.04 | 777.5 | −176.6 | 2.6 |
| XDH-14 | 14.98 | 777.0 | −174.9 | 2.6 |
| XDH-15 | 16.11 | 776.5 | −179.8 | 3.2 |
| XDH-16 | 17.04 | 776.0 | −186.5 | 2.6 |
| XDH-17 | 18.13 | 775.5 | −185.1 | 2.5 |
| XDH-18 | 18.98 | 775.0 | −190.9 | 2.6 |
| XDH-19 | 19.92 | 777.5 | −186.2 | 3.0 |
| XDH-20 | 20.97 | 777.0 | −183.6 | 2.4 |
| XDH-21 | 21.96 | 776.5 | −191.7 | 3.0 |
| XDH-22 | 23.12 | 776.0 | −187.5 | 2.6 |
| XDH-23 | 24.13 | 772.5 | −192.0 | 2.7 |
| XDH-24 | 25.15 | 772.0 | −181.0 | 2.2 |
| XDH-25 | 26.72 | 771.5 | −187.3 | 2.4 |
| XDH-26 | 27.86 | 771.0 | −189.8 | 2.6 |
| XDH-27 | 28.92 | 770.5 | −190.9 | 2.6 |
| XDH-28 | 29.82 | 770.0 | −180.9 | 2.7 |
| XDH-29 | 30.64 | 769.5 | −188.4 | 2.4 |
| XDH-30 | 32.03 | 769.0 | −187.6 | 3.0 |
| XDH-31 | 33.03 | 768.5 | −189.7 | 2.6 |
| XDH-32 | 34.04 | 768.0 | −178.1 | 2.7 |
| XDH-33 | 35.05 | 767.5 | −183.7 | 2.6 |
| XDH-34 | 36.05 | 767.0 | −189.4 | 2.4 |
| XDH-35 | 37.02 | 766.5 | −189.9 | 3.4 |
| XDH-36 | 37.94 | 766.0 | −188.5 | 3.2 |
| XDH-37 | 38.90 | 765.5 | −191.0 | 2.8 |
| XDH-38 | 39.65 | 765.0 | −186.5 | 2.4 |
| XDH-39 | 40.58 | 764.5 | −186.9 | 3.0 |
| XDH-40 | 41.54 | 764.0 | −194.7 | 2.6 |
| XDH-41 | 42.65 | 763.5 | −187.3 | 2.7 |

[a] The age is based on $^{230}$Th age of 783 ± 14 at the depth of 2.15 cm, and annual density bands of coral.

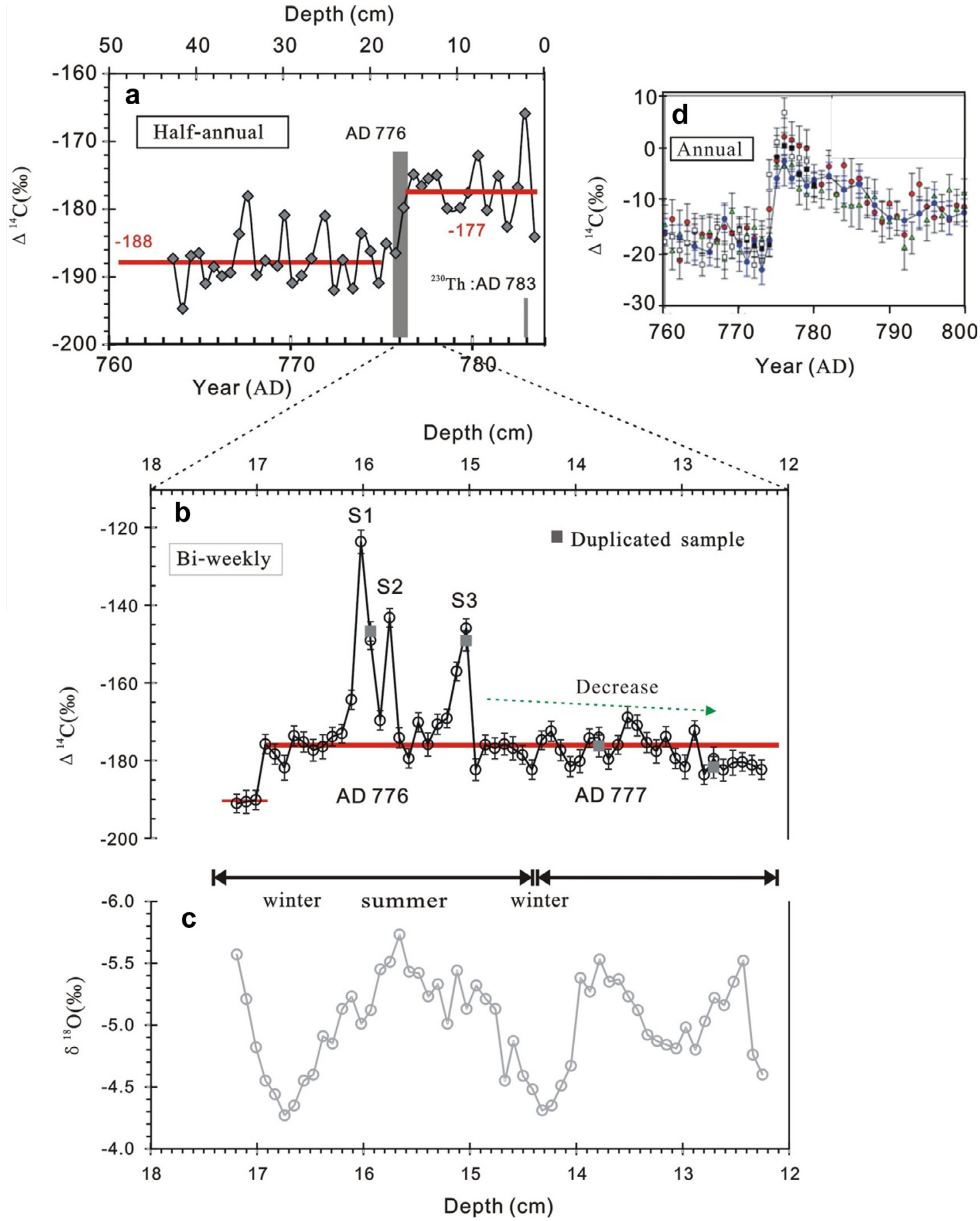


**Fig. 3.** $^{14}C$ spike event at AD 776 and AD 777 recorded in coral with half annual resolution (a), biweekly resolution (b). Coral $\delta^{18}O$ suggested the event occurred in winter or early spring of AD 776 (c). And the event documented by annual tree rings from south and north hemisphere (d, modified from [12]). S1, S2 and S3 indicate the peak and two smaller $^{14}C$ spikes in the event.

decreased slightly in AD 777. The three $\Delta^{14}C$ spikes occur in the summer of AD 776 probably represent the "peak time" of only one abrupt $^{14}C$ increase event. Reason for the drop of $\Delta^{14}C$ in the peak time remains unknown, maybe because of the influence from different carbon source in the oceanic environment or the fluctuation of the event itself.

The abrupt $^{14}C$ increase of ~45‰ in $\Delta^{14}C$ within two weeks has never been observed in tree rings from other sites before (Fig. 3d). In annual resolution tree rings records, ~15‰ increase of $\Delta^{14}C$ is found in the $^{14}C$ spike event [16], very similar to the half-annual resolution record in the coral. In addition to the stronger $^{14}C$ spike, the bi-weekly resolution also reflects a shorter spike time within half a year. The fact that the $^{14}C$ signal observed both in global tree rings and coral likely suggested an extraterrestrial origin of the event cause.

### 3.3. Bi-weekly resolution of coral $\delta^{18}O$

Coral $\delta^{18}O$ is strongly influenced by the precipitation/evaporation ratio. The higher $\delta^{18}O$ value appears in winter while the lower $\delta^{18}O$ value in summer [17–19]. Though the mean annual $\delta^{18}O$ values are close, the high-resolution record states the difference in the variation of $\delta^{18}O$ value in AD 776 and AD 777. Coral $\delta^{18}O$ in summer (June to August) of AD 776 almost stays in −5.00‰ to −5.50‰. But in the summer of AD 777, there is an obviously positive shift to −4.75‰ of coral $\delta^{18}O$. A difference of 0.45‰ of coral $\delta^{18}O$ exists between the summer of AD 776 and AD 777, which is not caused by the measuring error. It is likely linked with weaker Asian monsoon during that time [20], which induced lower precipitation/evaporation ratio in the summer of AD 777. The higher precipitation/evaporation ratio in the summer of AD 776 may be helpful for the $^{14}CO_2$ exchanging between atmosphere and sea water, and finally entering into coral and recorded.

## 4. Conclusions

Pre-heating method can improve the quality of $^{14}C$ preparation in labs of pollution. It guarantees the higher resolution of $^{14}C$ dating in the $^{14}C$ lab in GIGCAS. The average drilling method is useful to divide the coral into bi-weekly resolution subsamples. Different from the tree ring $^{14}C$ record in annual resolution, the bi-weekly resolution $^{14}C$ record in the coral shows a spike of 45‰ in $\Delta^{14}C$, and two smaller spikes with $\Delta^{14}C > 20‰$ within half a year. According to the coral $\delta^{18}O$, the $^{14}C$ spike event occurs in the summer of AD 776. High-resolution dating of $^{14}C$ in coral is a useful supplement to the tree ring document in investigating the mysterious abrupt $^{14}C$ increase during AD 776 and AD 777, which totally suggests an extraterrestrial origin of the event cause.

## Acknowledgments

We thank the project of Chinese Academy of Sciences Equipment Function Development and Technological Innovation (YZ2011046) and the State Key Laboratory of Isotope Geochemistry (SKLIG-KF-12-01, SKLIG-KF-12-02 and SKLIG-JY-12-01) for financial support. We are particularly gratefully to Dr. Xiaomei Xu in UC, Irvine who helps us a lot in AMS-$^{14}C$ measurement of the coal, OXI standards.

## References

[1] A. Mahadevan, An analysis of bomb radiocarbon trends in the Pacific, Mar. Chem. 73 (2001) 273.

[2] J.M. Lough, A strategy to improve the contribution of coral data to high-resolution palaeoclimatology, Palaeogeogr. Palaeoclimatol. Palaeoecol. 204 (2004) 115.

[3] F. Miyake, K. Nagaya, K. Masuda, T. Nakamura, A signature of cosmic-ray increase in AD 777–775 from tree rings in Japan, Nature 486 (2012) 240.

[4] Y. Liu, Z.F. Zhang, Z.C. Peng, M.X. Ling, C. Shen, W.G. Liu, X.C. Sun, C.D. Shen, K.X. Liu, W.D. Sun, Mysterious abrupt carbon-14 increase in coral contribution by a comet, Sci. Rep. 4 (2014) 3728.

[5] I.G. Usoskina, G.A. Kovaltsov, The carbon-14 spike in the 8th century was not caused by a cometary impact on Earth, Icarus (2014), http://dx.doi.org/10.1016/j.icarus.2014.06.009.

[6] A.L. Melott, Comment on "Mysterious abrupt carbon-14 increase in coral contributed by a comet", Yi Liu, et al., arXiv:1401.7276 (astro-ph.EP).

[7] V.V. Hambaryan, R. Neuhäuser, A galactic short gamma-ray burst as cause for the $^{14}C$ peak in AD777/5, Mon. Not. R. Astron. Soc. 430 (2013) 32.

[8] B.C. Thomas, A.L. Melott, K.R. Arkenberg, B.R. Snyder, Terrestrial effects of possible astrophysical sources of an AD777–775 increase in C-14 production, Geophys. Res. Lett. 40 (2014) 1237.

[9] A.L. Melott, B.C. Thomas, Causes of an AD 777–775 $^{14}C$ increase, Nature 491 (2012) 11695.

[10] I.G. Usoskin, B. Kromer, F. Ludlow, J. Beer, M. Friedrich, G.A. Kovaltsov, S.K. Solanki, L. Wacker, The AD775 cosmic event revisited: the Sun is to blame, Astron. Astrophys. 552 (2013) L3.

[11] T. Mitsuguchi, H. Kitagawa, E. Matsumoto, Y. Shibata, M. Yoneda, T. Kobayashi, T. Uchida, N. Ahagon, High-resolution $^{14}C$ analyses of annually-banded coral skeletons from Ishigaki Island, Japan: implications for oceanography, Nucl. Instr. Meth. B 223–224 (2004) 455.

[12] H. Kiagawa, T. Masuzawa, T. Makamura, E. Matsumoto, A batch preparation method for graphite targets with low level background for AMS $^{14}C$ measurements, Radiocarbon 35 (1993) 295.

[13] X.M. Xu, S.E. Trumbore, S.H. Zheng, J.R. Southon, K.E. McDuffee, M. Luttgen, J.C. Liu, Modifying a sealed tube zinc reduction method for preparation of AMS graphite targets: reducing background and attaining high precision, Nucl. Instr. Meth. B 259 (2007) 320.

[14] S. Szidat, T.M. Jenk, H.W. Gäggeler, H.A. Synal, I. Hajdas, G. Bonani, M. Saurer, THEODORE, a two-step heating system for the EC/OC determination of radiocarbon ($^{14}C$) in the environment, Nucl. Instr. Meth. B 223–224 (2004) 829.

[15] X.M. Xu, C.D. Shen, A.K. Stills, J.R. Southon, Homogeneity evaluation of Chinese sugar carbon (CSC) standard for AMS $^{14}C$ measurement, Nucl. Instr. Meth. B 259 (2013) 430.

[16] A.J.T. Jull, I.P. Panyushkina, T.E. Lange, V.V. Kukarshih, V.S. Myglan, K.J. Clark, M.W. Salzer, G.S. Burr, S.W. Leavitt, Excursions in the $^{14}C$ record at A.D.777–775 in tree rings from Russia and America, Geophys. Res. Lett. 41 (2014), http://dx.doi.org/10.1002/2014GL059874.

[17] T. Corrège, Sea surface temperature and salinity reconstruction from coral geochemical tracers, Palaeogeogr. Palaeoclimatol. Palaeoecol. 232 (2006) 408.

[18] D.H. Sun, M.K. Gagan, H. Cheng, H.S. Gagan, C.A. Dykoski, R.L. Edwards, R.X. Su, Seasonal and interannual variability of the Mid-Holocene East Asian monsoon in coral $\delta^{18}O$ records from the South China Sea, Earth Planet. Sc. Lett. 237 (2005) 69.

[19] R.X. Su, D.H. Sun, J. Bloemendal, Z.Y. Zhu, Temporal and spatial variability of the oxygen isotopic composition of massive corals from the South China Sea: influence of the Asian monsoon, Palaeogeogr. Palaeoclimatol. Palaeoecol. 240 (2006) 630.

[20] P.Z. Zhang, H. Cheng, R.L. Edwards, F.H. Chen, Y.J. Wang, X.L. Yang, J. Liu, M. Tan, X.F. Wang, J.H. Liu, C. An, Z.B. Dai, J. Zhou, D.Z. Zhang, J.H. Jia, L.Y. Jin, K. Johnson, Science 322 (2008) 940.